

# Hydrogen as Carbon Gasifying Agent During Glycerol Steam Reforming over Bimetallic Co-Ni Catalyst

Chin Kui Cheng, Rwi Hau Lim, Anabil Ubil, Sim Yee Chin, Jolius Gimbut

Faculty of Chemical & Natural Resources Engineering, Universiti Malaysia Pahang, Kuantan, Malaysia  
Email: [chinkui@ump.edu.my](mailto:chinkui@ump.edu.my)

Received 2012

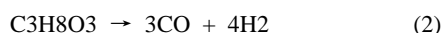
## ABSTRACT

Alumina-supported bimetallic cobalt-nickel catalyst has been prepared and employed in a fixed-bed reactor for the direct production of synthesis gas from glycerol steam reforming. Physicochemical properties of the 5Co-10Ni/85Al<sub>2</sub>O<sub>3</sub> catalyst were determined from N<sub>2</sub>-physisorption, H<sub>2</sub>-chemisorption, CO<sub>2</sub> and NH<sub>3</sub>-temperature-programmed desorption measurements as well as X-ray diffraction analysis. Both weak and strong acid sites are present on the catalyst surface. The acidic:basic ratio is about 7. Carbon deposition was evident at 923 K; addition of H<sub>2</sub> however has managed to reduce the carbon deposition. Significantly, this has resulted in the increment of CH<sub>4</sub> formation rate, consistent with the increased carbon gasification and methanation. Carbon deposition was almost non-existent, particularly at 1023 K. In addition, the inclusion of hydrogen also has contributed to the decrease of CO<sub>2</sub> and increase of CO formation rates. This was attributed to the reverse water-gas-shift reaction. Overall, both the CO<sub>2</sub>:CO and CO<sub>2</sub>:CH<sub>4</sub> ratios decrease with the hydrogen partial pressure.

**Keywords:** Carbon Deposition; Catalyst; Gasification; Glycerol; Steam Reforming

## 1. Introduction

The use of renewable feedstock is fast gaining attention in lieu of the context of securing sustainable use of energy and preserving the environment for the future generations. Considerable effort has been devoted into applying green catalytic route to convert renewable feedstock such as biomass into commodity chemicals and clean bio-fuels. In particular, glycerol, also known as 1,2,3-propanetriol, is produced in excess quantity in the form of by-product during biodiesel synthesis. It constitutes an approximately 10wt% of the total product. In an effort to add value to glycerol as precursor for renewable and clean energy production, it was steam-reformed at temperatures greater than 773 K to produce H<sub>2</sub>, CO and CO<sub>2</sub> which are important ingredients for the manufacture of a variety of industrial chemicals [1,2]. The relevant reactions are:



Carbon deposition is a perennial issue during glycerol steam reforming. Cheng et al. [3] have reported a kinetic study of carbon deposition during glycerol steam reforming over alumina supported bimetallic Co-Ni catalyst. At least two types of carbonaceous species were deposited on the catalyst surface [3]. Sanchez and Comelli [4] published a paper on deactivation process and regeneration technique during glycerol steam reforming over a Ni-alumina catalyst. A TPO characterized by a main peak centered at 963 K was obtained [4].

As a continuation to the previous works, this paper reports on the adoption of H<sub>2</sub> as co-reactant during glycerol steam reforming to encourage simultaneous carbon gasification. Results on the effects of H<sub>2</sub> addition towards carbon deposition and product variation will be presented and elucidated in detailed.

## 2. Methodology

### 2.1. Catalyst Synthesis and Physicochemical Characterization

Bimetallic 5Co-10Ni/85Al<sub>2</sub>O<sub>3</sub> catalyst was prepared via co-impregnation of cobalt and nickel nitrate solutions on  $\gamma$ -alumina which has been preheated at 873 K for 6 h. Subsequently, the slurry catalyst was oven-dried at 403 K for overnight and then calcined at 873 K for 6 h to obtain oxide metals. For the physicochemical characterization, BET surface area and pore volume were obtained from liquid N<sub>2</sub> physisorption on the Quantachrome Autosorb-1 unit. The metal catalyst dispersion and surface area were determined from Micromeritics ASAP 2000 via H<sub>2</sub>-chemisorption technique. The crystallography of catalyst was examined via XRD technique via scan rate of 4° min<sup>-1</sup> from 10° to 80°. Carbon content of collected samples post-reforming reaction, was determined using a Shimadzu Solid Sample Module (SSM-5000A) based on combustion at 1173 K.

### 2.2. Reaction Studies

Figure 1 shows the experimental set-up for the current experimental work. Reaction runs were conducted in a stainless-steel fixed bed reactor under minimal influence from physical transport limitations. 60 wt% aqueous glycerol solution was prepared and directly injected into a 10-mm diameter fixed-bed reactor system using 50 mL syringe pump reacting at temperatures between 923 and 1023 K. Prior to reaction, catalyst was reduced in-situ using 50 ml min<sup>-1</sup> of H<sub>2</sub> for 2 h. Subsequently, H<sub>2</sub> was co-added to the reactor as gasifying reactant. Total GHSV for the experiment was controlled at 5×10<sup>4</sup> mL g<sup>-1</sup> h<sup>-1</sup>.

For fixed-bed reactor operation with no recycle stream, Levenspiel [5] shows that the reaction rate is governed by:

$$-r_A = (y_{A,feed} \times F_{feed} \times X) / m \quad (3)$$

where  $-r_A$  = reaction rate of reactant A ( $\text{mol s}^{-1} \text{g}_{\text{cat}}^{-1}$ )

$y_{A,feed}$  = mole fraction of component A in the reactant stream

$F_{feed}$  = total molar flowrate ( $\text{mol s}^{-1}$ )

$X$  = conversion of species A

$m$  = mass of catalyst ( $\text{g}_{\text{cat}}$ )

For the purpose of comparison with other catalysts, specific activity, defined as the rate of reaction per unit active area offers a better index. Thus, for metal-catalysed reactions such as steam reforming, the weight-based rate was divided by the active metal area (obtained from  $\text{H}_2$ -chemisorption) to give the specific reaction rate of the catalyst. Hence,

$$\hat{r}_i = \frac{r_i}{SA_{\text{calc}}} \quad (4)$$

where  $\hat{r}_i$  = specific reaction rate of species  $i$  ( $\text{mol m}^{-2} \text{s}^{-1}$ )

$r_i$  = reaction rate of species  $i$  ( $\text{mol s}^{-1} \text{g}_{\text{cat}}^{-1}$ )

$SA_{\text{calc}}$  = metal surface area ( $\text{m}^2 \text{g}_{\text{cat}}^{-1}$ )

### 3. Results and Discussion

#### 3.1. Physicochemical Properties of Fresh Catalysts

As shown in **Table 1**, fresh calcined catalyst exhibits BET surface area and pore volume of  $166 \text{ m}^2 \text{g}_{\text{cat}}^{-1}$  and  $0.57 \text{ cm}^3 \text{g}_{\text{cat}}^{-1}$  respectively. The dispersion of metal was rather low, probably

due to the high metal loading (15 wt%) employed in the current study.  $\text{H}_2$ -chemisorption analysis revealed that the average particle diameter was 136.0 nm with metal surface area of  $0.74 \text{ m}^2 \text{g}_{\text{cat}}^{-1}$ .  $\text{NH}_3$ - and  $\text{CO}_2$ -TPD measurements revealed the existence of two peaks, representing both strong and weak acid/basic sites (cf. **Table 2**). Overall, the concentration of acid site was higher than the basic site in ratio ranging from 7.0 to 7.3.

The diffractogram shown in **Figure 2** for calcined catalyst indicates the presence of  $\text{Co}_3\text{O}_4$  and  $\text{NiCo}_2\text{O}_4$  at  $2\theta = 33.0^\circ$ , and an overlapped peak consisting of  $\text{CoAl}_2\text{O}_4$  and  $\text{NiAl}_2\text{O}_4$  at  $38.0^\circ$ . In addition, the two peaks at  $2\theta$  of  $44.0^\circ$  and  $46.5^\circ$  for the bi-metallic catalyst may be attributed to the existence of  $\text{NiO}$ ,  $\text{NiAl}_2\text{O}_4$  and  $\text{CoAl}_2\text{O}_4$ . The small peak at  $2\theta = 59.0^\circ$  represents  $\text{NiAl}_2\text{O}_4$  and  $\text{CoAl}_2\text{O}_4$  phase. Furthermore, another small diffraction peak at  $2\theta$  of  $62.0^\circ$  is attributed to  $\text{NiO}$ . The peak at  $2\theta = 65.0^\circ$  corresponds to the presence of composites of  $\text{Co}_3\text{O}_4$  and  $\text{CoAl}_2\text{O}_4$  while the diffraction peak at  $68.0^\circ$  is assigned to  $\text{NiAl}_2\text{O}_4$ .

#### 3.2. Reaction Studies

Reaction results in **Figure 3** show that with the addition of  $\text{H}_2$ , the  $\text{CO}_2$  and  $\text{CO}$  formation rates varied in reverse trend suggesting that the presence of  $\text{H}_2$  in the feed encouraged the reverse water-gas-shift, viz.  $\text{H}_2 + \text{CO}_2 \leftrightarrow \text{CO} + \text{H}_2\text{O}$ . In addition, it seems that the  $\text{CH}_4$  formation rates increased with  $P_{\text{hydrogen}}$  indicating an increase in methane production activity.

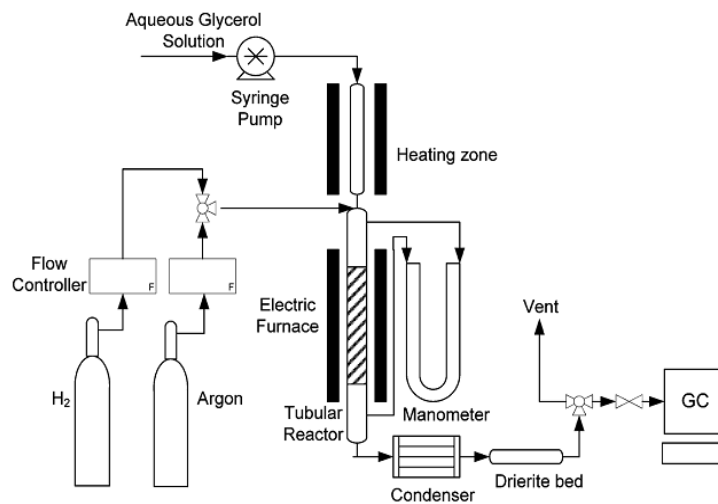


**Figure 1.** Experimental set up for glycerol steam reforming.

**Table 1.** Physicochemical attribute of calcined bimetallic Co-Ni/ $\text{Al}_2\text{O}_3$  catalyst.

| Properties   | 5Co-10Ni/85Al <sub>2</sub> O <sub>3</sub> |
|--|---|
| BET surface area ( $\text{m}^2 \text{g}_{\text{cat}}^{-1}$ )   | 166                                       |
| Pore volume ( $\text{cm}^3 \text{g}_{\text{cat}}^{-1}$ )       | 0.57                                      |
| Dispersion (%)   | 0.74                                      |
| Metal surface area ( $\text{m}^2 \text{g}_{\text{cat}}^{-1}$ ) | 0.74                                      |
| Active particle diameter (nm)                                  | 136.0                                     |

**Table 2.** Acid/ base properties of fresh Co-Ni/ $\text{Al}_2\text{O}_3$  catalyst.

| Properties   | 5Co-10Ni/85Al <sub>2</sub> O <sub>3</sub> |
|--|---|
| $\text{NH}_3$ heat of desorption, ( $\text{kJ mol}^{-1}$ ) | 35.5                                      |
|  | 87.3                                      |
| $\text{CO}_2$ heat of desorption, ( $\text{kJ mol}^{-1}$ ) | 62.4                                      |
|  | 56.0                                      |
| Acid concentration ( $\mu\text{mol m}^{-2}$ )              | 1.50                                      |
|  | 2.90                                      |
| Basic concentration ( $\mu\text{mol m}^{-2}$ )             | 0.21                                      |
|  | 0.42                                      |

Subsequently, the product ratios ( $\text{CO}_2:\text{CO}$ ,  $\text{CO}_2:\text{CH}_4$  and  $\text{CO}:\text{CH}_4$ ) as a function of  $P_{\text{hydrogen}}$  showed that the  $\text{CO}_2:\text{CO}$  ratio is practically constant with  $P_{\text{hydrogen}}$  as a result of reverse-water-gas-shift reaction (cf. **Figure 4**). The ratio was lower than unity indicating that CO formation rate was higher than  $\text{CO}_2$  as the latter was being consumed to produce the former.  $\text{CO}_2:\text{CH}_4$  decreased with  $P_{\text{hydrogen}}$  due to the increased  $\text{CH}_4$  formation rate, whilst the ratio  $\text{CO}:\text{CH}_4$  decreased because the increase in  $\text{CH}_4$  formation rate was higher than the increase recorded for CO formation rate.

### 3.3. Carbon Deposition

**Figure 5** suggests a decrease in carbon deposition rate with  $\text{H}_2$  partial pressure, in particular at 923 K. This observation is consistent with the increase in  $\text{CH}_4$  formation rate indicating that both methanation and carbon gasification contributed to the increase in  $\text{CH}_4$  formation. However, temperature seems to play an increasingly dominant role in reducing carbon laydown than adding  $\text{H}_2$  gasifying reactant at temperatures  $\geq 973$  K. At 1023 K, deposition of carbon was essentially zero.

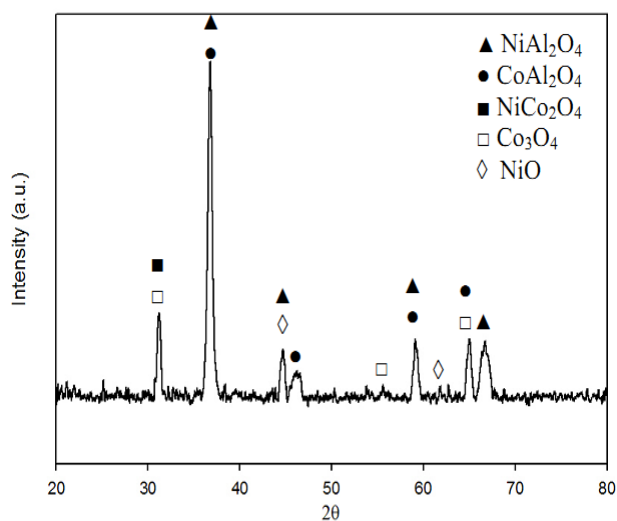


**Figure 2.** XRD pattern of calcined Co-Ni/ $\text{Al}_2\text{O}_3$  catalyst.

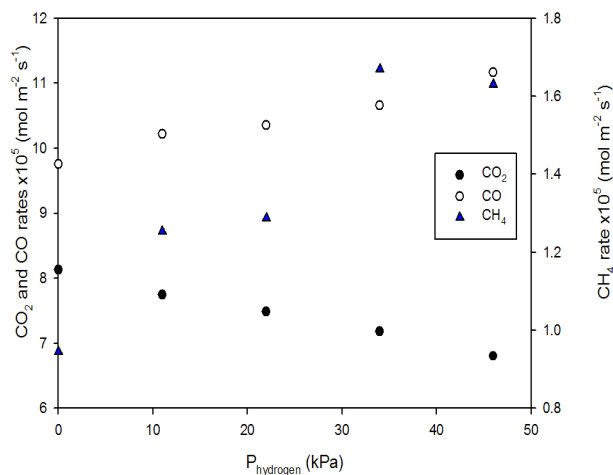


**Figure 3.** Effect of  $P_{\text{hydrogen}}$  on product formation rates at 973 K.

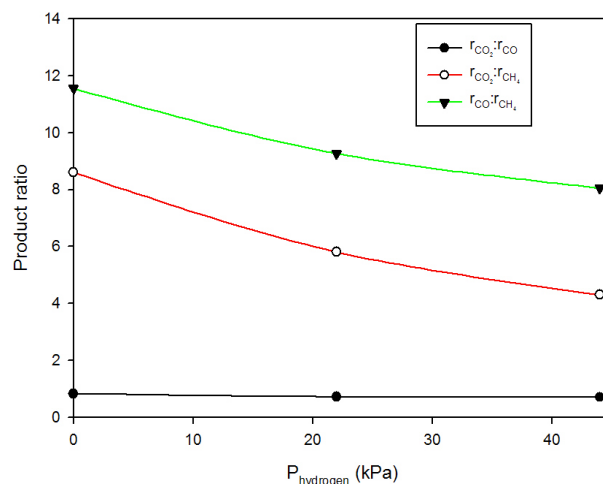


**Figure 4.** Effect of  $P_{\text{hydrogen}}$  on product ratios at 973 K.

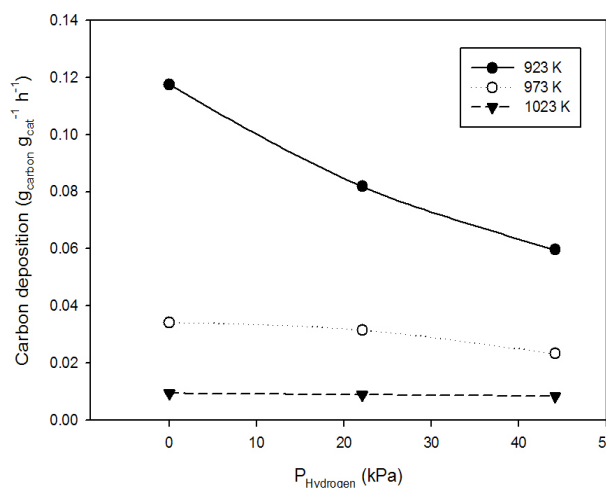


**Figure 5.** Effect of  $P_{\text{hydrogen}}$  on carbon laydown as function of temperature.

## 4. Conclusions

The effects of adding  $\text{H}_2$  gasifying reactant during the glycerol steam reforming have been examined. Reaction data revealed that  $\text{H}_2$  addition led to the increased  $\text{CH}_4$  formation which can be attributed to the gasification of carbon and methanation. In addition, the product formation rate of  $\text{CO}_2$  decreased due to reverse water-gas-shift.

## 5. Acknowledgements

Authors would like to thank Universiti Malaysia Pahang for the provision of short-term grant to fund this project.

## REFERENCES

- [1] S. Adhikari, S. Fernando, and A. Haryanto, "A comparative thermodynamic and experimental analysis on hydrogen production by steam reforming of glycerin," *Energy Fuels*, vol. 21, pp. 2306–2310.
- [2] C. K. Cheng, S. Y. Foo, and A. A. Adesina, "Glycerol steam

- reforming over bimetallic Co-Ni/Al<sub>2</sub>O<sub>3</sub>,” *Ind. Eng. Chem. Res.*, vol. 49, pp. 10804–10817.
- [3] C. K. Cheng, S. Y. Foo, and A. A. Adesina, “Carbon deposition on bimetallic Co-Ni/Al<sub>2</sub>O<sub>3</sub> catalyst during steam reforming of glycerol,” *Catal. Today*, vol. 164, pp. 268–274.
- [4] E. A. Sanchez, and R. A. Comelli, “Hydrogen by glycerol steam reforming on a nickel-alumina catalyst: Deactivation processes and regeneration,” *Int. J. Hydrogen Energy*, in press.
- [5] O. Levenspiel, *Chemical Reaction Engineering*. New York: John Wiley & Sons, 1999.